Steel and Composite Structures, *Vol. 16, No. 2 (2014) 117-133*
DOI: http://dx.doi.org/10.12989/scs.2014.16.2.117

Analysis of dynamic behavior for truss cable structures

Wen-Fu Zhang *, Ying-Chun Liu, Jing Ji and Zhen-Chao Teng

Heilongjiang Key Laboratory of Disaster Prevention, Mitigation and Protection Engineering, College of Civil and Architecture Engineering, Northeast Petroleum University, Daqing 163318, P.R. China

(*Received July 05, 2012, Revised September 09, 2013, Accepted September 24, 2013*)

Abstract. Natural vibration of truss cable structures is analyzed based upon the general structural analysis software ANSYS, energy variational method and Rayleigh method, the calculated results of three methods are compared, from which the characteristics of free-vibration are obtained. Moreover, vertical seismic response analysis of truss cable structures is carried out via time-history method. Introducing three natural earthquake waves calculated the results including time-history curve of vertical maximal displacement, time-history curve of maximal internal force. Variation curve of maximal displacement of node along span, and variation curve of maximal internal force of member along span are presented. The results show the formulas of frequencies for truss cable structures obtained by energy variational method are of high accuracy. Furthermore, the maximal displacement and the maximal internal force occur near the 1/5 span point. These provide convenient and simple design method for practical engineering.

Keywords: truss cable structures; energy variational method; natural vibration; time-history analysis; finite element analysis

1. Introduction

Cable-suspended structure is a kind of reasonable force structural system, and is widely applied in long-span sport building and bridge. Among the parallel span systems, a cable truss (see Fig. 1) is a counter-stressed double-cable system in which the top and bottom chords consist of continuous pre-stressed cables anchored at each end, and between which numerous light rigid spacers are placed to provide the web members (Raoof and Davies 2004, Ma *et al*. 2011). It has better shape stability, and that is earliest adopted in Stockholm Skating Museum which is designed by the Swedish engineer Jawerth in 1966, then is widely applied in all countries. Moreover, many scholars have researched the static and dynamic characteristics of cable truss (Kassimali and Parsi-Feraidoonian 1987, Kmet and Kokorudova 2006, Kmet 2009, Vlajić and Kostić 2010, Ma 2011). But, a truss cable (see Fig. 2) which will be studied in this paper is different from a cable truss, which is a suspended structure that can replace flexible cables, and consists of curved solid-web or latticed members that have a certain bending rigidity and compress rigidity. Internal force of the chords is mainly tension when subjecting uniformly distributed loads (Shen *et al*. 2006). It has the virtues of flexible cables and light-weight steel structures. The virtues and wide applications have been received great attentions domestically. Truss cable structures have been

*Corresponding author, Professor, E-mail: zwfdqpi@126.com

http://www.techno-press.org/?journal=scs&subpage=8 ISSN: 1229-9367 (Print), 1598-6233 (Online)

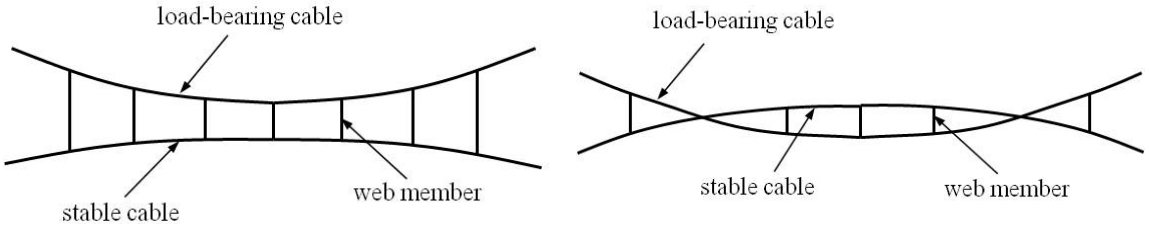

Fig. 1 Layout of cable truss

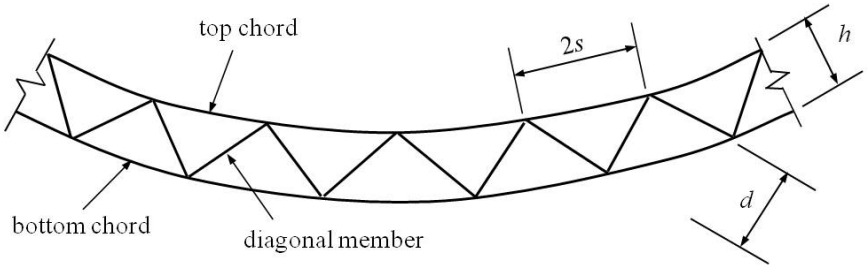

Fig. 2 Layout of truss cable

earlier applied to the practical engineering abroad, such as Yokohama Plant Stadium (Japan, 1960), Tokyo Yoyogi Sports Centre (Japan, 1964), The 22nd Olympic Games Natatorium (Former Soviet Union, 1980). The importance and application in practical engineering prompt the development of theoretical and experimental research. Professor Shi-Zhao and Chong-Bao (Shen *et al*. 2006), Ye and Xu (1994), Liu (2002) etc. have studied static behavior of truss cables and acquired many important conclusions, but there is little research to dynamic behavior. Consequently, it is very important and fundamental to understand the behavior of truss cable structures.

2. Basic data and assumptions

According to the present code, this paper designs a 40-meter-span truss cable, the ratio of sag to span is 1/12, the height of cross section is 0.5 m, area of upper and lower members is both 20.4 cm^2, area of diagonal member is 3.57 cm^2, elastic modulus is $2.06 \times 10^{11} N/m^2$, bending rigidity is $5.253 \times 10^7 N \cdot m^2$, shearing rigidity is $1.904 \times 10^7 N$, gravity load representation value is 285.58 kN, mass of unit length is 728.53 kg/m. The axial shape of truss cable is like parabola.

Basic assumptions (Zhang 2005, Shen *et al*. 2006) are the following:

(1) Material characteristic accords to Hooke's law.
(2) Small sag and only vertical loads is considered.
(3) The ratio of curvature radius to height of cross section accords to small curvature assumption, i.e., $R/h >> 5$.
(4) For latticed members, continuum method should be applied. Equivalent section area, inertia moment, and shearing rigidity are calculated by the rule of equal rigidity. Torsional moment of inertia is ignored. Eq. (1) is their formulas.

$$\left.\begin{aligned} A &= A_a + A_b \\ I &= \frac{A_a A_b}{F} h^2 \\ GA &= \frac{EA_d h^2 s}{d^3} \end{aligned}\right\} \tag{1}$$

where, A_a, A_b are area of upper and lower chords, respectively, h is the height of cross section, I is equivalent inertia moment of truss cable, GA is equivalent shearing rigidity, A_d is area of diagonal member, d is the length of diagonal member, s is half of space between upper chord segment (Liu 2002). Layout of truss cable is shown in Fig. 2.

3. Finite element model

Truss cable structure can be simplified to a plane truss consisted of hinges and struts. The material is linear, elastic and isotropic. According to the principle of equivalent force, the load is transformed to node load. Deflection accords to the principle of small deflection. In this paper, element type of model is Link1, which is a uniaxial tension-compression element with two degrees of freedom at each node. According to axial equation and geometry of truss cable and the height of cross section, we can educe the equations and nodal coordinates of upper and lower chords. Then, lower chord between 3-53 nodes is divided to 25 elements, i.e., the length of each element is 1.5 m, the length of 1-3 node and 53-55 node is 1.25 m, then elements are created base on the nodes. Restrictions are applied to 1 and 55 nodes. For vibration analysis, concentrated mass model is used, in which MASS21 element is placed on nodes (Zhang 2005). The model by ANSYS software is shown in Fig. 3.

4. Natural vibration analysis

4.1 Natural vibration analysis by FEM

ANSYS is the large general finite element structural analysis software. Modal analysis in ANSYS can be used to natural vibration characteristics analysis of structure. There are four parts

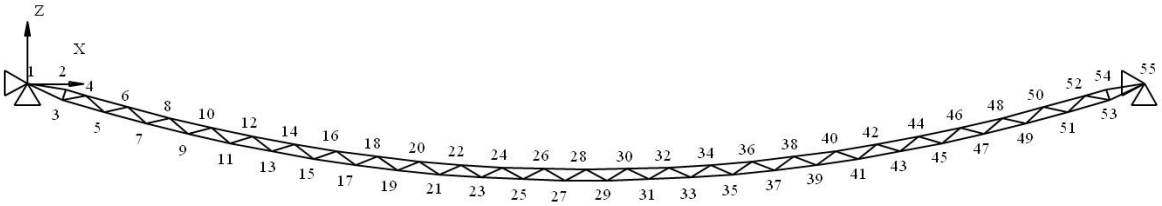

Fig. 3 Truss cable structure finite element model

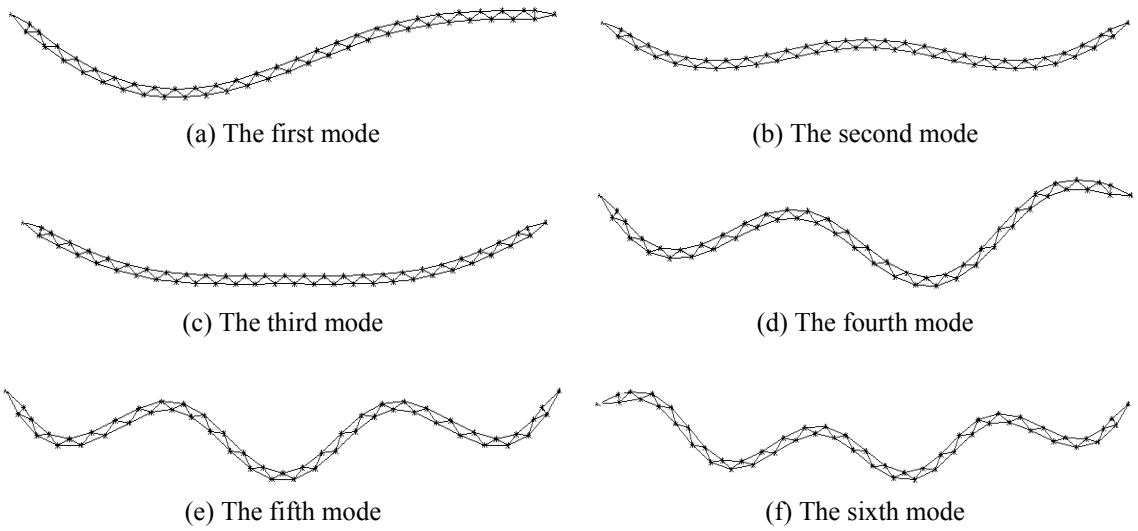

(a) The first mode (b) The second mode

(c) The third mode (d) The fourth mode

(e) The fifth mode (f) The sixth mode

Fig. 4 The fist six modes of truss cable by ANSYS

(establishment of model, loads and solution, expansion of modes, observation of results) in analysis. Then the process of analysis is detailedly given. Finite element model is established above. Analysis type is modal, and subspace method is applied to extract modes. Effect load in modal analysis is only zero displacement restriction. Where, restrictions are applied in direction x and z, then solution is done. Last, the frequency and vibration mode can be obtained by expanding modes (Seo *et al*. 2010). It is noted that the unit of obtained frequency in ANSYS is Hz, the first six frequencies are given in Table 1 after multiplied 2π. The first six modes obtained by ANSYS are shown in Fig. 4. Seen from it, the first mode is also an antisymmetric mode.

4.2 Natural vibration analysis by the energy variational method (*EVM*)

We assume the initial shape of truss cable is

$$z_0 = \frac{4fx}{l}\left(1-\frac{x}{l}\right) \tag{2}$$

where, f, l are respectively the sag and span of truss cable.

Dynamic displacement is

$$\left.\begin{aligned} w(x,t) &= W(x)\sin(\omega t+\varphi) \\ \theta(x,t) &= \Theta(x)\sin(\omega t+\varphi) \end{aligned}\right\} \tag{3}$$

Mode function is

$$\left.\begin{aligned} W(x) &= \sum_{m=1}^{P} A_m \sin\frac{m\pi x}{l} \\ \Theta(x) &= \sum_{m=1}^{P} B_m \cos\frac{m\pi x}{l} \end{aligned}\right\} \tag{4}$$

where, m = 2, 4, 6, … , p = 2, 4, 6, … , for antisymmetric mode,

m = 1, 3, 5, … , p = 3, 5, 7, … , for symmetric mode

In the case of small amplitude vertical vibration, total potential energy (Clough and Penzien 2006, Chopra 2007) can be written as

$$\Pi = \frac{1}{2}\left(\frac{EA}{l}\right)\left[0\int_0^l\left(\frac{\partial z_0}{\partial x}\cdot\frac{\partial W}{\partial x}\right)dx\right]^2 + \frac{EI}{2}\int_0^l\left(\frac{d\Theta}{dx}\right)^2 dx + \frac{GA}{2}\int_0^l\left(\frac{dW}{dx}-\Theta\right)^2 dx - \frac{\overline{m}\,\omega^2}{2}\int_0^l W^2 dx \tag{5}$$

where, $\overline{m}$ is uniformly distributed mass, ω is frequency of truss cable.

By substituting Eq. (3), Eq. (4) into Eq. (5), we can get the implicit expression for Π (omitted here for limit space).

According to theory of the minimum of total potential energy, $\frac{\partial \Pi}{\partial A_m} = 0$, $\frac{\partial \Pi}{\partial B_m} = 0$

$$\begin{aligned} &A_m\left[\frac{64EAf^2}{l^3\pi^2}\left(\frac{1-\cos m\pi}{m}\right)^2 + \frac{GA\pi^2m^2}{2l} - \overline{m}\,\omega^2\left(\frac{l}{2}\right)\right] \\ &+ \sum_{i=1(i\neq m)}^{p} A_i\frac{64EAf^2}{l^3\pi^2}\cdot\frac{(1-\cos m\pi)(1-\cos i\pi)}{im} - B_m GA\left(\frac{m\pi}{2}\right) = 0 \end{aligned} \qquad (m = 1,2,3,\ldots,p) \tag{6}$$

$$B_m\left(\frac{m^2EI\pi^2}{2l} + \frac{GAl}{2}\right) - A_m GA\left(\frac{m\pi}{2}\right) = 0 \qquad (m = 1,2,3,\ldots,p) \tag{7}$$

From Eq. (6) and Eq. (7), we can get

$$B_m = A_m\frac{m\pi GAl}{m^2EI\pi^2 + GAl^2} \tag{8}$$

$$\begin{aligned} &A_m\left[2\overline{A}_0\left(\frac{1-\cos m\pi}{m}\right)^2 + \frac{GA\pi^2m^2}{l^2} - \frac{(GA)^2(m\pi)^2}{m^2EI\pi^2 + GAl^2} - \overline{m}\,\omega^2\right] \\ &+ \sum_{i=1(i\neq m)}^{p} A_i\overline{A}_0\frac{2(1-\cos m\pi)(1-\cos i\pi)}{im} = 0 \end{aligned} \tag{9}$$

where, $\overline{A}_0 = \frac{64EAf^2}{l^4\pi^2}$, $(m,i = 1,2,3,\cdots,p)$, set

$$\overline{C}_m = 2\overline{A}_0\left(\frac{1-\cos m\pi}{m}\right)^2 + \frac{GA\pi^2m^2}{l^2} - \frac{(GA)^2(m\pi)^2}{m^2EI\pi^2 + GAl^2}$$

then, Eq. (9) can be expressed in the following form

$$A_m\left[\overline{C}_m - \overline{m}\,\omega^2\right] + \sum_{i=1(i\neq m)}^{p} A_i \overline{A}_0 \frac{2(1-\cos m\pi)(1-\cos i\pi)}{im} = 0 \tag{10}$$

As an example, set $p = 7$, then the explicit expression of symmetric vibration (m, i = 1, 3, 5, 7) is as follow

$$\begin{matrix} m=1 \\ m=3 \\ m=5 \\ m=7 \end{matrix}\begin{bmatrix} \overline{C}_1 - \overline{m}\,\omega^2 & \frac{8}{3}\overline{A}_0 & \frac{8}{5}\overline{A}_0 & \frac{8}{7}\overline{A}_0 \\ \frac{8}{3}\overline{A}_0 & \overline{C}_3 - \overline{m}\,\omega^2 & \frac{8}{15}\overline{A}_0 & \frac{8}{21}\overline{A}_0 \\ \frac{8}{5}\overline{A}_0 & \frac{8}{15}\overline{A}_0 & \overline{C}_5 - \overline{m}\,\omega^2 & \frac{8}{35}\overline{A}_0 \\ \frac{8}{7}\overline{A}_0 & \frac{8}{21}\overline{A}_0 & \frac{8}{35}\overline{A}_0 & \overline{C}_7 - \overline{m}\,\omega^2 \end{bmatrix}\begin{Bmatrix} A_1 \\ A_3 \\ A_5 \\ A_7 \end{Bmatrix} = \begin{Bmatrix} 0 \\ 0 \\ 0 \\ 0 \end{Bmatrix} \tag{11}$$

For antisymmetric vibration (m, i = 2, 4, 6, 8), set $p = 8$,

$$\begin{matrix} m=2 \\ m=4 \\ m=6 \\ m=8 \end{matrix}\begin{bmatrix} \overline{C}_2 - \overline{m}\,\omega^2 & 0 & 0 & 0 \\ 0 & \overline{C}_4 - \overline{m}\,\omega^2 & 0 & 0 \\ 0 & 0 & \overline{C}_6 - \overline{m}\,\omega^2 & 0 \\ 0 & 0 & 0 & \overline{C}_8 - \overline{m}\,\omega^2 \end{bmatrix}\begin{Bmatrix} A_2 \\ A_4 \\ A_6 \\ A_8 \end{Bmatrix} = \begin{Bmatrix} 0 \\ 0 \\ 0 \\ 0 \end{Bmatrix} \tag{12}$$

Then, for antisymmetric mode frequency can be simply written as

$$\omega_m^2 = \frac{\overline{C}_m}{\overline{m}} = \frac{m}{\overline{m}l}\left[\frac{mGA\pi^2}{l} - \frac{m(GA)^2\pi^2 l}{m^2 EI\pi^2 + GAl^2}\right] \qquad (m = 2,4,6,...) \tag{13}$$

Next, the first three symmetric and antisymmetric frequency formulas and derivations will be presented in more detail.

(1) The first three symmetric mode:

(a) For $p = 1$, $m = 1$, mode function is

$$\left.\begin{aligned} W(x) &= A_1 \sin\frac{\pi x}{l} \\ \Theta(x) &= B_1 \cos\frac{\pi x}{l} \end{aligned}\right\} \tag{14}$$

from Eq. (10), we can get

$$A_1(\overline{C}_1 - \overline{m}\,\omega_1^2) = 0 \tag{15}$$

Therefore, the frequency formula of one-half sine wave symmetric mode can be expressed as

$$\omega_1^2 = \frac{2}{\overline{m}l}\left[\frac{256EAf^2}{\pi^2 l^3} + \frac{GA\pi^2}{2l} - \frac{(GA)^2\pi^2 l}{2(EI\pi^2 + GAl^2)}\right] \tag{16}$$

(b) For $p = 3$, $m = 1, 3$, mode function is

$$\left.\begin{aligned} W(x) &= A_1 \sin\frac{\pi x}{l} + A_3 \sin\frac{3\pi x}{l} \\ \Theta(x) &= B_1 \cos\frac{\pi x}{l} + B_3 \cos\frac{3\pi x}{l} \end{aligned}\right\} \tag{17}$$

from Eq. (11), we can get

$$\begin{bmatrix} \overline{C}_1 - \overline{m}\omega_3^2 & \frac{8}{3}\overline{A}_0 \\ \frac{8}{3}\overline{A}_0 & \overline{C}_3 - \overline{m}\omega_3^2 \end{bmatrix} \begin{Bmatrix} A_1 \\ A_3 \end{Bmatrix} = \begin{Bmatrix} 0 \\ 0 \end{Bmatrix} \tag{18}$$

$$\det\begin{vmatrix} \overline{C}_1 - \overline{m}\omega_3^2 & \frac{8}{3}\overline{A}_0 \\ \frac{8}{3}\overline{A}_0 & \overline{C}_3 - \overline{m}\omega_3^2 \end{vmatrix} = 0 \tag{19}$$

Solving Eq. (19), we can get the frequency formula of three-half sine wave symmetric mode.

$$\omega_3^2 = \frac{(\overline{C}_1 + \overline{C}_3) \pm \sqrt{(\overline{C}_1 - \overline{C}_3)^2 + \frac{256}{9}\overline{A}_0^2}}{2\overline{m}} \tag{20}$$

where, $\overline{C}_3 = \dfrac{512EAf^2}{9\pi^2 l^4} + \dfrac{9GA\pi^2}{l^2} - \dfrac{9(GA)^2\pi^2}{9EI\pi^2 + GAl^2}$.

or $p = 5$, $m = 1, 3, 5$, mode function is

$$\left.\begin{aligned} W(x) &= A_1 \sin\frac{\pi x}{l} + A_3 \sin\frac{3\pi x}{l} + A_5 \sin\frac{5\pi x}{l} \\ \Theta(x) &= B_1 \cos\frac{\pi x}{l} + B_3 \cos\frac{3\pi x}{l} + B_5 \cos\frac{5\pi x}{l} \end{aligned}\right\} \tag{21}$$

from Eq. (11), we can get

$$\begin{bmatrix} \overline{C}_1 - \overline{m}\omega_5^2 & \frac{8}{3}\overline{A}_0 & \frac{8}{5}\overline{A}_0 \\ \frac{8}{3}\overline{A}_0 & \overline{C}_3 - \overline{m}\omega_5^2 & \frac{8}{15}\overline{A}_0 \\ \frac{8}{5}\overline{A}_0 & \frac{8}{15}\overline{A}_0 & \overline{C}_5 - \overline{m}\omega_5^2 \end{bmatrix} = \begin{Bmatrix} 0 \\ 0 \\ 0 \end{Bmatrix} \tag{22}$$

By solving the eigenvalue of matrix, we can get the frequency of five-half sine wave symmetric mode.

(2) The first three antisymmetric mode:

(a) For $p = 2$, $m = 2$, mode function is

$$\left.\begin{aligned} W(x) &= A_2 \sin\frac{2\pi x}{l} \\ \Theta(x) &= B_2 \cos\frac{2\pi x}{l} \end{aligned}\right\} \tag{23}$$

from Eq. (13), we can get

$$\omega_2^2 = \frac{2}{\overline{m}l}\left[\frac{2GA\pi^2}{l} - \frac{2(GA)^2\pi^2 l}{4EI\pi^2 + GAl^2}\right] \tag{24}$$

(b) For $p = 4$, $m = 4$, mode function is

$$\left.\begin{aligned} W(x) &= A_4 \sin\frac{4\pi x}{l} \\ \Theta(x) &= B_4 \cos\frac{4\pi x}{l} \end{aligned}\right\} \tag{25}$$

from Eq. (13), we can get

$$\omega_4^2 = \frac{4}{\overline{m}l}\left[\frac{4GA\pi^2}{l} - \frac{4(GA)^2\pi^2 l}{16EI\pi^2 + GAl^2}\right] \tag{26}$$

(c) For $p = 6$, $m = 6$, mode function is

$$\left.\begin{aligned} W(x) &= A_6 \sin\frac{6\pi x}{l} \\ \Theta(x) &= B_6 \cos\frac{6\pi x}{l} \end{aligned}\right\} \tag{27}$$

from Eq. (13), we can get

$$\omega_6^2 = \frac{6}{\overline{m}l}\left[\frac{6GA\pi^2}{l} - \frac{6(GA)^2\pi^2 l}{36EI\pi^2 + GAl^2}\right] \tag{28}$$

The first six frequencies of vibration are calculated by these formulas, and listed in Table 1.

4.3 Natural vibration analysis by Rayleigh method (RM)

Mode function is

Table 1 Comparison of the first six frequencies

Frequency (1/s)	FEM	EVM	Difference	RM	Difference	Numbers of half wave
1	6.102	6.405	4.97%	6.405	4.97%	2
2	12.239	12.364	1.02%	14.874	21.53%	3
3	17.046	18.196	6.75%	16.208	4.92%	1,3
4	22.854	23.474	2.71%	23.474	2.71%	4
5	33.896	34.851	2.82%	34.803	2.68%	5
6	46.917	45.771	2.51%	45.771	2.51%	6

$$\left.\begin{aligned} W(x) &= A\sin\frac{m\pi x}{l} \\ \Theta(x) &= B\cos\frac{m\pi x}{l} \end{aligned}\right\} \tag{29}$$

According to Rayleigh method, we get

$$\omega^2 = \frac{1}{\overline{m}}\left[\frac{128EAf^2}{\pi^2 l^4}\left(\frac{1-\cos m\pi}{m}\right)^2 + \frac{GA\pi^2}{l^2}m^2 - \frac{(GA)^2(m\pi)^2}{EI\pi^2 m^2 + GAl^2}\right] \qquad (m = 1,2,3,\ldots,p) \tag{30}$$

The first six frequencies of vibration by this method are listed in Table 1. Furthermore, we plot the first six mode shapes of truss cable obtained by three methods (FEM, EVM, RM) in Figs. 5-10. From them, we can see clearly that mode shapes of three methods are very similar except the third mode. It is noted that the third mode as well as the second mode is also coupling of single and three sine half waves, it can be a kind of phenomena of insert frequency. From Table 1, the differences of frequencies by EVM are very little. The differences of second and third mode frequency by RM are big. This can be explained as that the assumed the mode function is not so good as others. For antisymmetric mode, the formula of frequency of EVM and RM is the same.

5. Time-history analysis under vertical earthquake simulation

5.1 Selection of earthquake waves

In time-history analysis, it is important to choose earthquake waves. There are three factors to be considered: earthquake intensity, earthquake spectrum characteristic and earthquake duration (Li *et al*. 2002). This paper selects three natural vertical earthquake waves — EL-Centro earthquake record, Taft earthquake record, Beijing Restaurant earthquake record. According to design earthquake of code for seismic design (China), peak value of earthquake wave is adjusted to 70 gal in time-history analysis. Acceleration peak value of EL-Centro earthquake record is 206.3 gal, duration is 5 s, time interval is 0.02 s. Acceleration peak value of Taft earthquake record is 102.9 gal, duration is 20 s, time interval is 0.02 s. Acceleration peak value of Beijing Restaurant earthquake record is 34.99 gal, duration is 40 s, time interval is 0.01 s. Acceleration records of three earthquake waves are shown in Fig. 11.

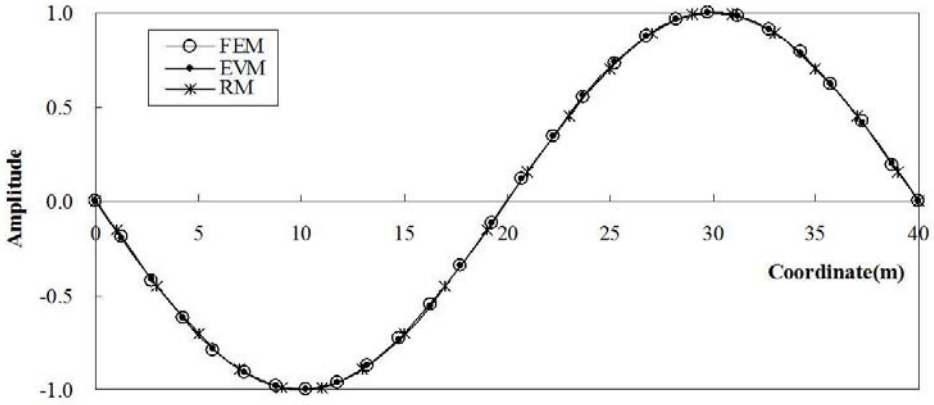

Fig. 5 First mode shape of truss cable by three methods

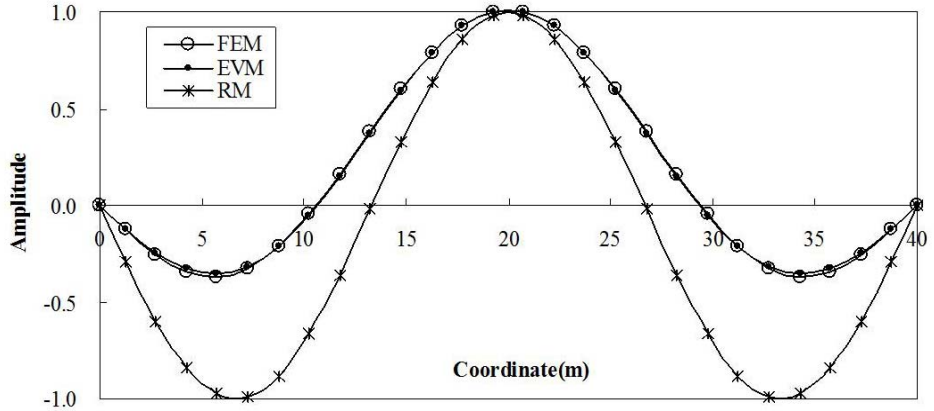

Fig. 6 Second mode shape of truss cable by three methods

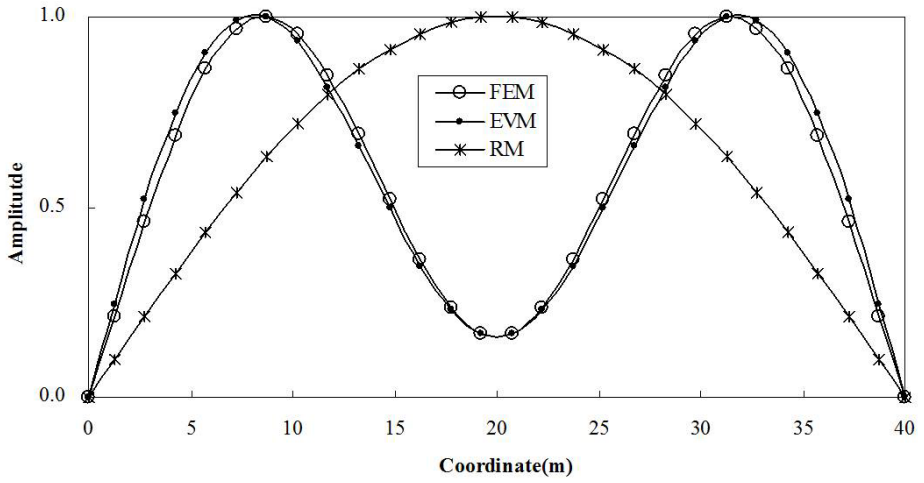

Fig. 7 Third mode shape of truss cable by three methods

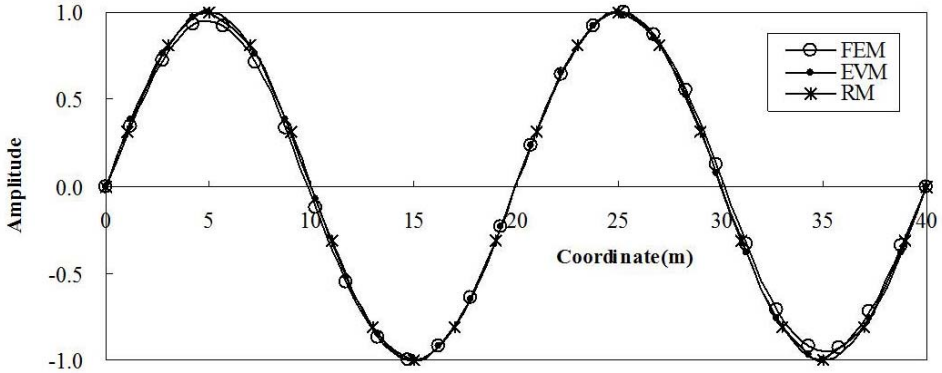

Fig. 8 Fourth mode shape of truss cable by three methods

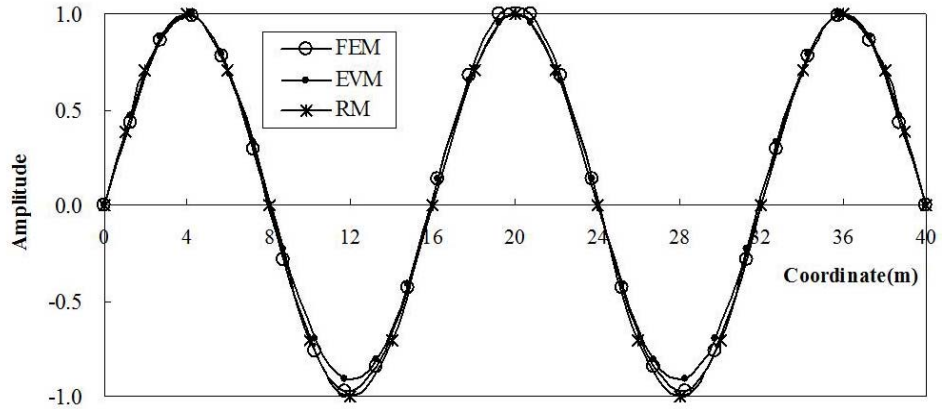

Fig. 9 Fifth mode shape of truss cable by three methods

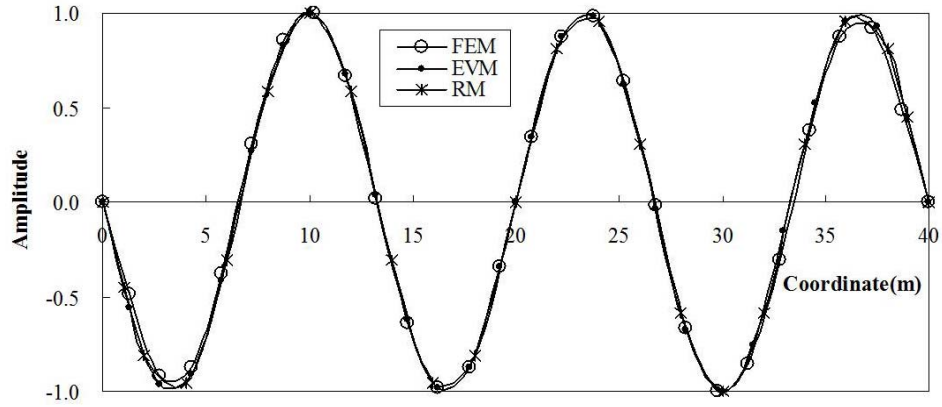

Fig. 10 Sixth mode shape of truss cable by three methods

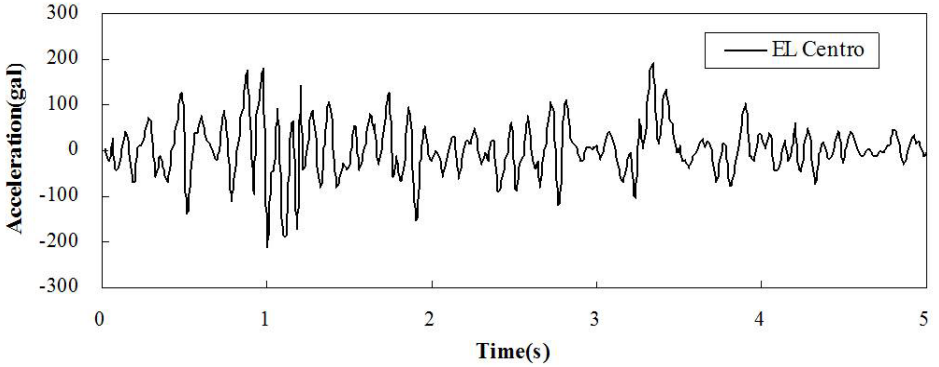

(a) EL Centro wave

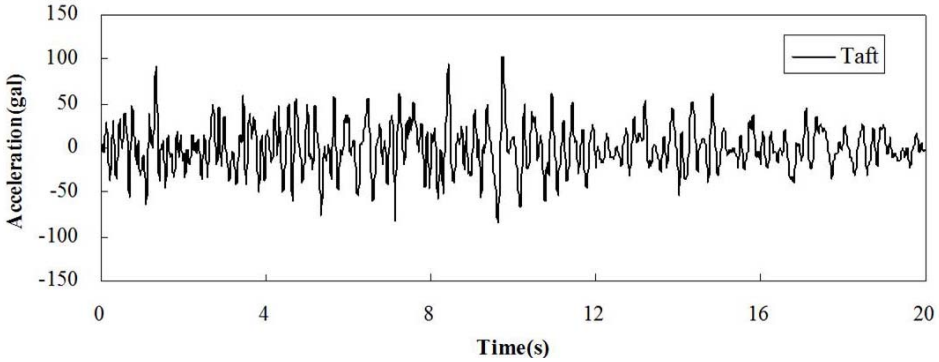

(b) Taft wave

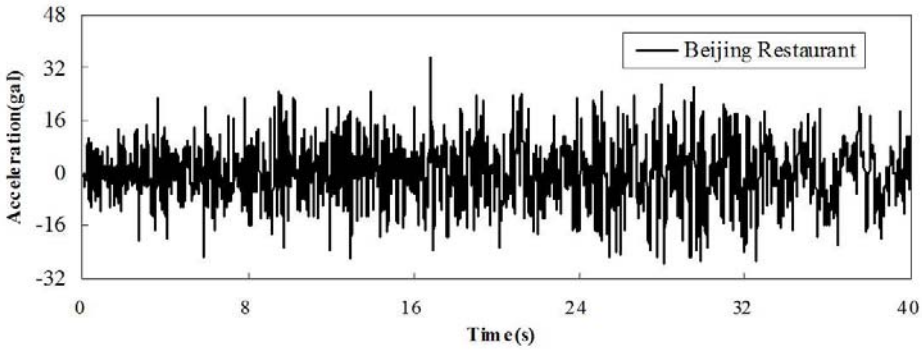

(c) Beijing Restaurant wave

Fig. 11 Vertical Acceleration records of three kinds of earthquake waves

5.2 Time-history response of nodal displacement and internal force

With APDL language of ANSYS program, data of acceleration record can be read to ANSYS by Table array. Time interval is 0.02 s. Damping ratio of cable structure is set to 0.02. The mass damp multiplier and the stiffness damp multiplier can be obtained by the first two vertical

Table 2 Maximal displacement and internal force

Wave	EL-Centro	Taft	Beijing Restaurant
Time (s)	1.96	9.88	29.77
Displacement (mm)	4.96	10.39	12.77
Internal force (kN)	33.91	72.94	87.97

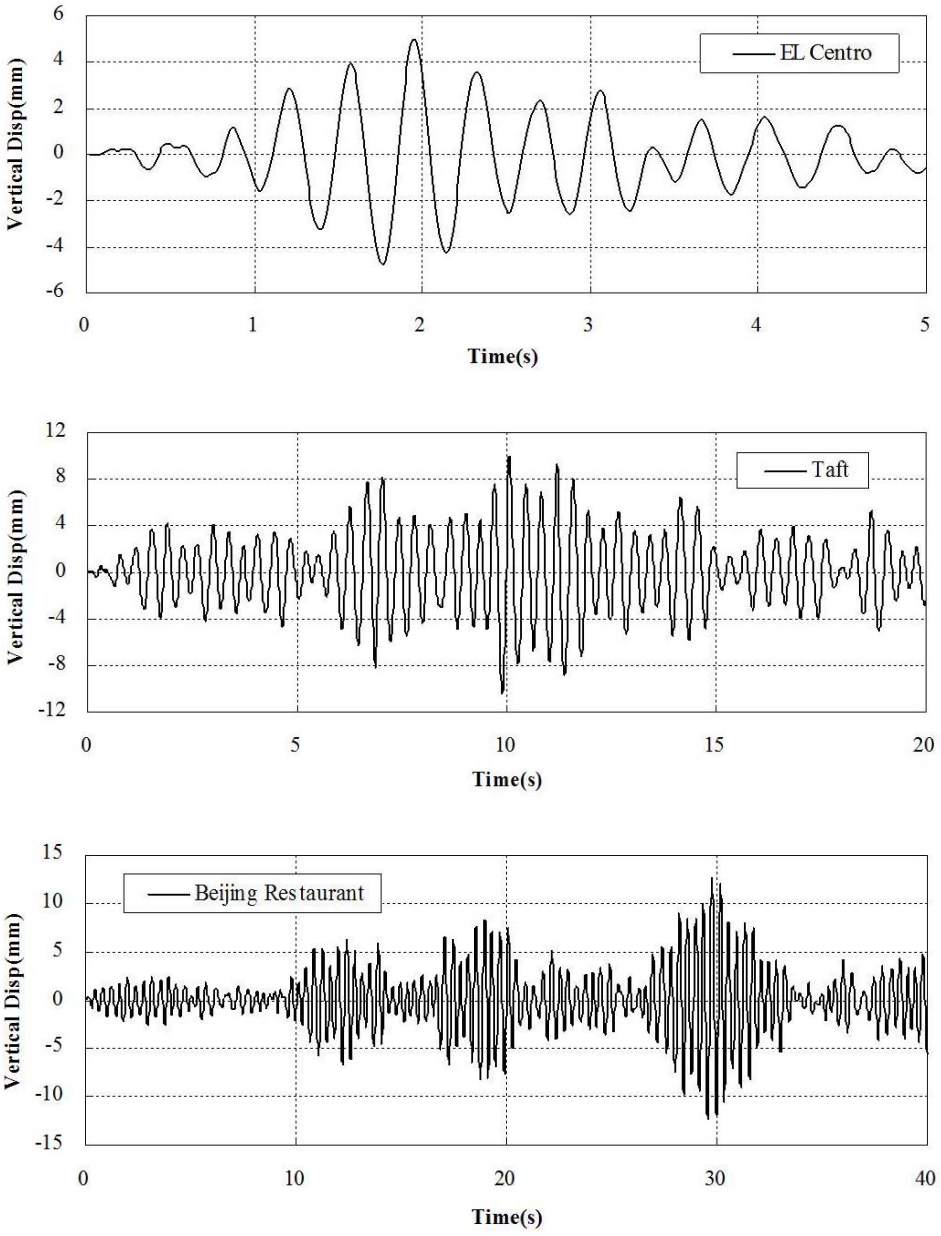

Fig. 12 Time history of vertical displacement for node12 under three kinds of earthquake waves

symmetric modes. i.e., α = 0.28496, β = 0.0137. Full method is applied to time-history analysis. By the analysis, we notice that the maximum displacement occurs near the 1/5 span point (node 12 or node 44) and the maximum internal force occurs near the 1/5 span (member 11-13 or member 43-45). Maximum values are tabulated in Table 2. Vertical displacement time history of node 12 curves under three kinds of earthquake waves are shown in Fig. 12. Internal force time history of member 11-13 curves under three kinds of earthquake waves are plotted in Fig. 13.

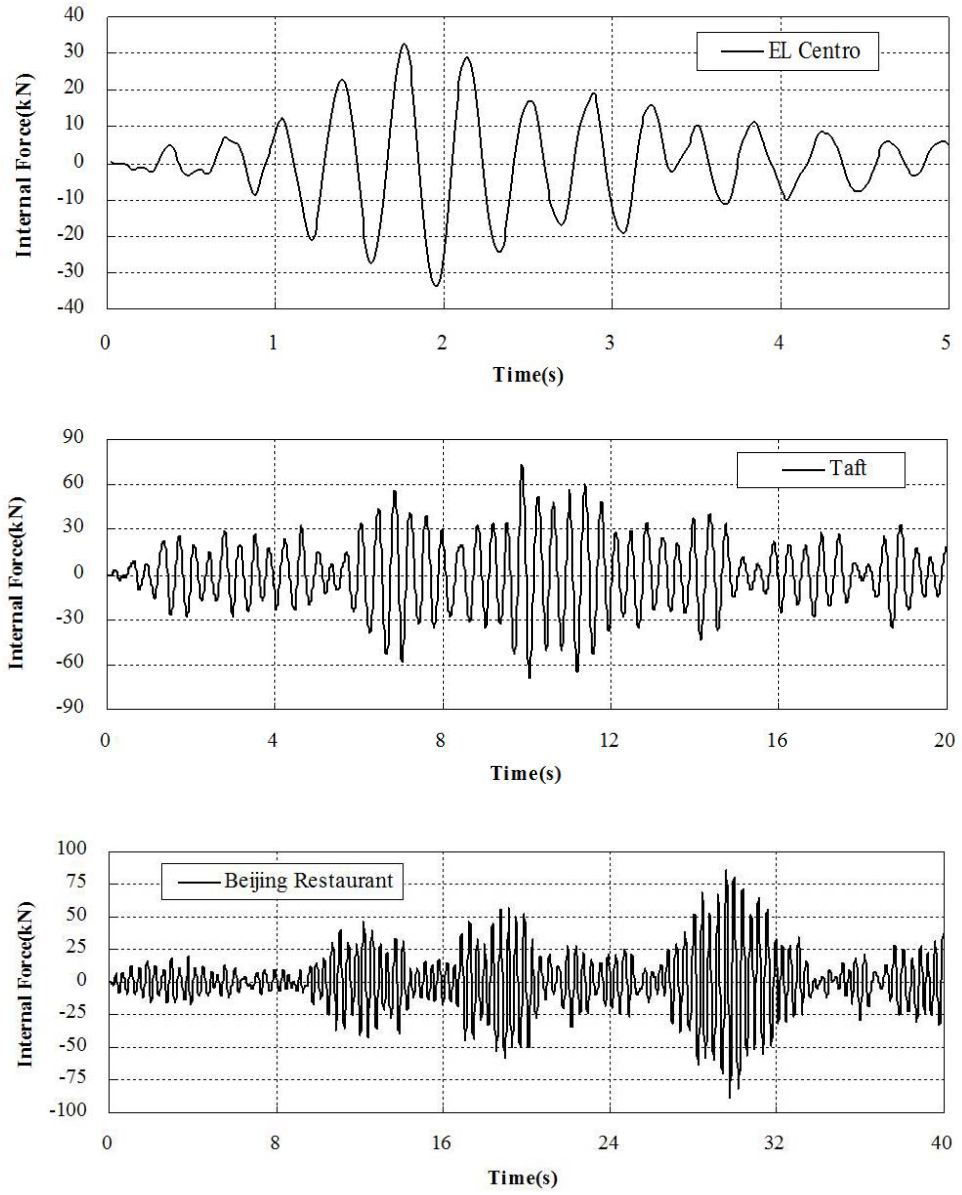

Fig. 13 Time history of vertical displacement for node12 under three kinds of earthquake waves

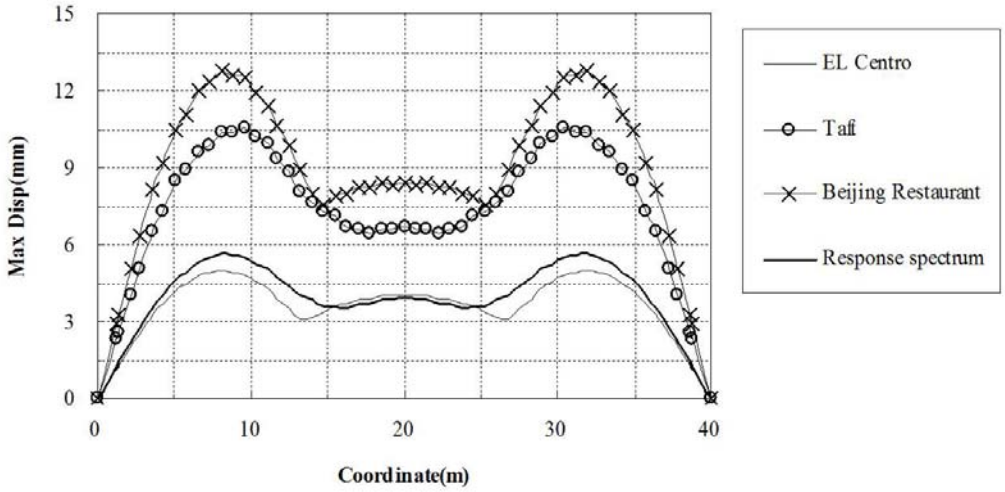

Fig. 14 Variation of maximal displacement along span

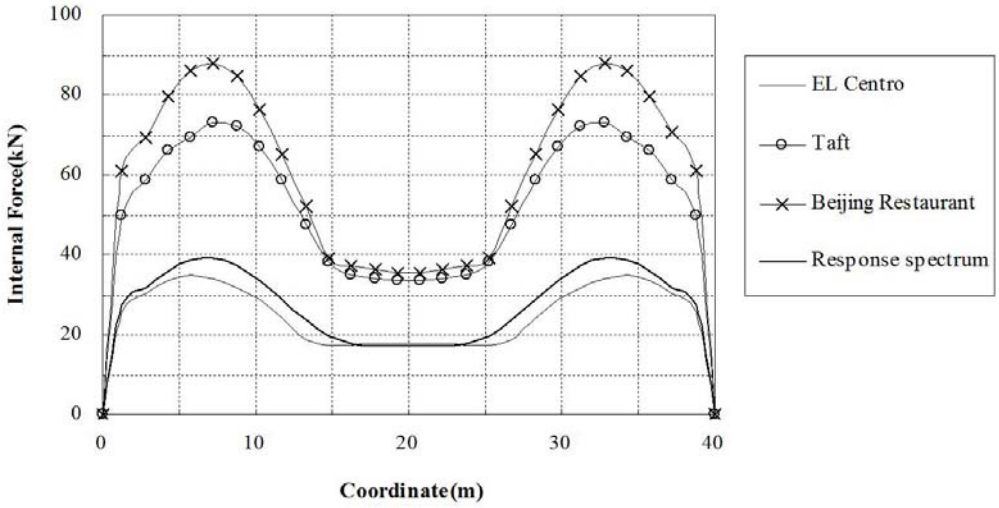

Fig. 14 Variation of maximal displacement along span

5.3 Variations of maximum displacement and internal force along span

Maximum displacement of each node and internal force of each member can be obtained by time-history analysis. Their variations along span are shown in Figs. 14 and 15. From these figures, we can find that under three kinds of earthquake waves, the results of EL Centro wave is close to that of mode decomposition response spectrum method (maximum displacement of node 12 is 5.62 mm, maximum force of member 11-13 is 38.94 kN). The results of Taft and Beijing Restaurant waves are bigger. Moreover, the seismic response of truss cable structure is smaller under EL-Centro earthquake simulation, the ratio of max vertical dynamic displacement to max

static displacement (82.91 mm) and that of max dynamic force to static force (401.8 kN) are all less than 1/10. It is proved that truss cable structure has strong rigidity.

6. Conclusions

Natural vibration for truss cable structure is analyzed by finite element methods, energy variational method and Rayleigh method. The frequencies of vibration of truss cable structure are compared. The first six mode shapes of truss cable are given. Moreover, vertical seismic response analysis of truss cable structures under different earthquake action is carried out by time-history method and analysis. Variation of node maximum displacement and member maximum internal force along span are obtained. The following conclusions are made.

(1) The theoretical formulas of frequencies obtained by energy variational method are of high accuracy, which can be conveniently used in practical project, especially in the preliminary design stage.
(2) The maximum displacement of node and the maximum internal force of member for truss cable structure occur near 1/5 span point under earthquake action, rather than in the span center of truss cable as expected. Same rule can be found in the distribution of maximum internal force of member. This phenomenon reminds engineers to pay enough attention in the design for long-span truss cable.

Acknowledgments

This work was financially supported by the National Natural Science Foundation of China (51178087).

References

Chopra, A.K. (Translated by Li-li Xie, Da-Gang Lv) (2007), *Dynamics of Structures: Theory and Applications to Earthquake Engineering*, (2nd Edition), Higher Education Press, Beijing, China.

Clough, R. and Penzien, J. (Translated by Guang-yuan Wang) (2006), *Dynamics of Structure*, (2nd Edition), Higher Education Press, Beijing, China.

Kassimali, A. and Parsi-Feraidoonian, H. (1987), "Nonlinear behavior of prestressed cable trusses", *J. Constr. Steel Res.*, **7**(6), 435-450.

Kmet, S. and Kokorudova, Z. (2006), "Nonlinear analytical solution for cable truss", *ASCE*, *J. Eng. Mech.*, **132**(1), 119-123.

Kmet, S. and Kokorudova, Z. (2009), "Non-linear closed-form computational model of cable trusses", *Int. J. Non-Linear Mech.*, **44**(7), 735-744.

Ye, J.H. and Xu, C.B. (1994), "Theoretical and parametric studies of the plane rigid-cable structures", *J. Harbin Archit.Civ. Eng. Inst.*, **27**(2), 38-43.

Li, G.Q., Li, J. and Su, X.Z. (2002), *Aseismatic Design for Building Structure*, China Architecture and Building Press, Beijing, China.

Liu, K.G. (2002), "Analysis of stiff cable structures", *Spatial Structures*, **8**(2), 19-25.

Ma, G.Y., Yao, Y.L. and He, J.P. (2011), "Dynamic characteristics of a new annular tensile cable-truss structure", *International Conference on Electric Technology and Civil Engineering*, Beijing, April.

Ma, X. (2011), "A nonlinear force method model for dynamic analysis of cable trusses", *Adv. Mater. Res.*,

250-253, 2281-2284.
Raoof, M. and Davies, T.J. (2004). "Influence of variations in the axial stiffness of steel cables on vertical deflections of cable trusses", *J. Constr. Steel Res.*, **60**(3-5), 411-420.
Seo, Y.G., Jeong, U.Y. and Cho, J.S. (2010), "Simplified finite element dynamic analysis of cable-supported structures subjected to seismic motions", *KSCE J. Civil Eng.*, **14**(4), 579-587.
Shen, S.Z., Xu, C.B., Zhao, C. and Wu, Y. (2006), *Cable Structure Design*, China Architecture and Building Press, Beijing, China.
Vlajić, L. and Kostić, D. (2010), "Theoretical-experimental static and dynamic analysis of double layered catenary", *Architect. Civil Eng.*, **8**(2), 169-175.
Zhang, W.F. (2005), *Spatial Structures*, Science Press, Beijing, China.
Zhang, W.F. and Liu, Y.C. (2005), "Dynamic response analysis for truss cable structures", *Proceedings of ICASS05 Fourth International Conference on Advances in Steel Structures*, Shanghai, June.

CC